Optimization of the polishing process on a polishing machine with horizontal overarm

Lukáš Veselý[1], *Ondřej* Matoušek[1,2], *Tomáš* Vít[1, 3*] and *Jan* Novosád[3]

[1]asphericon s.r.o., 463 12 Jeřmanice, Czechia
[2]Technical university of Liberec, Institute of New Technologies and Applied Informatics, 461 17 Liberec, Czechia
[3]Technical University of Liberec, Dept. of Power Engineering Equipment, 461 17 Liberec, Czechia

Abstract. Understanding the basic principles of polishing on machines with autorotating swing kinematics is important for the description and understanding of more advanced polishing technologies. The article deals with the theoretical and numerical analysis of the polishing process and its comparison with the experiment performed during the real process on the machine. The dependence of the mutual position of the tool and workpiece axes on the removal distribution within the polished surface was described and demonstrated

1 Polishing process overview

Polishing is a chemical-mechanical machining of the workpiece surface. The goal is to get a smooth, flawless surface that also meets the shape requirements. Usually during polishing, one of the two parts (tool or product) rotates, while the other part oscillates. Polishing is the final and most precise machining operation, during which the surface of the lens can still be handled. [1, 2].

The basic equation which describes the dependence of the removal rate on process parameters is the Preston equation [3]:

$$\frac{d\xi}{dt} = k_p p v_R, \qquad (1)$$

where ξ is the thickness of the material layer removed, t is the polishing time, p is the pressure acting on the polished element at a given location, v_r is the relative velocity between the polishing tool and the workpiece and k_p is Preston constant.

The validity of the relationship mentioned above was confirmed in many works. Currently, theoretical research focuses on evaluating the influence of chemical and mechanical factors on the polishing process. Details and analysis of individual approaches can be found in [4].

This article aims to show the influence of individual members of Preston equation on the final removal rate of material in the case of polishing with overarm.

1.1 Preston constant

The magnitude of the Preston constant depends on various parameters. According to [4, 5], the Preston constant is affected by the friction coefficient between the workpiece / slurry / and the pad. It is also affected by the friction mod. The magnitude of the Preston constant also depends significantly on the hardness of the machined surface, chemical composition of polishing slurry, character and size of polish grains.

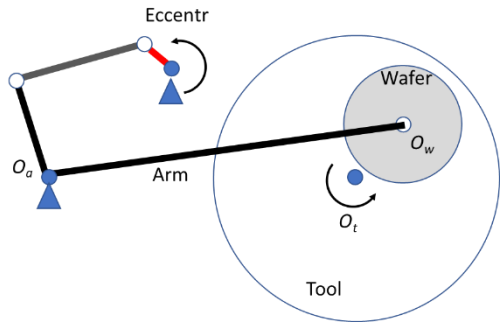

Fig. 1. Layout of NC polishing machine with horizontal overarm.

1.2 Modes of polishing

It is possible to distinguish between three modes of polishing based on interaction between the polishing pad/slurry and workpiece. In the case of so-called contact mode, there is direct contact between the polishing pad and the workpiece. No stable fluid film is formed between the workpiece and the tool, so no pressure gradient is created. This mode occurs at low relative velocity and high pressure. The coefficient of friction is in the range of 0.1.

In the hydroplaning mode (Fig. 2), a constant film of fluid is formed between the workpiece and the tool. Unlike the previous one, this mode is characterized by a high value of relative velocity and a relatively low value of pressure. The coefficient of friction typically ranges from 0.001 to 0.01. The pressure distribution in hydroplaning mode is highly dependent on the attack angle, i.e., the wedge between the workpiece and the tool. The third possible mode is mixing or transition mode,

* Corresponding author: tomas.vit@tul.cz

which arises in unstable states between the two modes mentioned above.

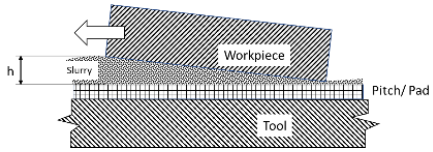

Fig. 2. Hydroplaning mode of polishing.

Results of experiments presented in [2] and [4] shows significant drop of the friction coefficient in the relative velocity range called Coulomb interval. In agreement with the previous mentioned modes the drop of friction coefficient is described as the aqua planning effect, characterized by the formation of a liquid film between the glass surface and the polishing pad because of the high rotational speed.

A technique for the measurement of the dynamic fluid film pressure during polishing was presented in [3]. It was found that the pressure distribution is significantly different between static and dynamic conditions.

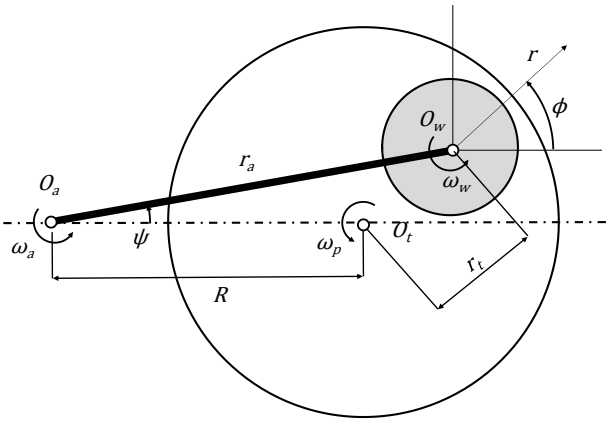

Fig. 3. Kinematics of the mechanism.

Stationary results showed an asymmetrical pressure distribution and some subatmospheric pressures. Dynamic experiments showed pressure increasing monotonically from edge to centre and no sub-atmospheric pressures.

1.3 Kinematics of polishing

The basic arrangement of the polishing process is described in [4]. Regarding the definition of individual components, as shown in Fig. 3 the following relationships can be specified.

The magnitude of the relative velocity is:

$$v_R = \{[r(\omega_w + \omega_a - \omega_t) + \omega_a r_a \cos\varphi - \omega_t r_t \cos\varphi]^2 + [\omega_a r_a \sin\varphi - \omega_t r_t \sin\varphi]^2\}^{1/2} \quad (2)$$

And corresponding torque on the wafer:

$$M_w = \int_0^{r_w}\int_0^{2\pi} \mu p r^2 \left[\frac{(\omega_a r_a - \omega_t r_t)\cos\varphi}{v_R} + \frac{r(\omega_w+\omega_a-\omega_t)}{v_R}\right] d\varphi dr \quad (3)$$

It is necessary to realize that both ω_a and r_t are time dependent harmonic functions generated by the motion of eccentric part of the mechanism.

It is obvious that for $\omega_w = \omega_t - \omega_a$ the torque of the workpiece is $M_w = 0$. In this case the relative velocity is independent on position r on the workpiece and the average relative velocity is uniform over whole surface of the workpiece.

In real operation, the connection between the arm and the workpiece body is realized via a ball joint. Additional torque is generated in the real process due to the friction in the ball joint. The torque M_w will therefore be nonzero and $\omega_w < \omega_t - \omega_a$.

1.4 Pressure distribution.

The pressure distribution between the workpiece and the tool can be described by the so-called Reynolds equation, which is derived for the flow of fluid in very narrow channels. Detailed analysis can be found in [4]

$$\frac{\partial}{\partial x}\left(\frac{h^3}{12\mu}\frac{\partial p}{\partial x}\right) + \frac{\partial}{\partial y}\left(\frac{h^3}{12\mu}\frac{\partial p}{\partial y}\right) = \frac{\partial}{\partial x}\left[\frac{h(u_{x,w}+u_{x,t})}{2}\right] + \frac{\partial}{\partial y}\left[\frac{h(u_{y,w}+u_{y,t})}{2}\right] - u_{x,w}\frac{\partial h}{\partial x} - u_{y,w}\frac{\partial h}{\partial y} \quad (4)$$

The analysis shows that the pressure distribution strongly depends on the value of wedge which is expressed by the change in gap thickness h over the workpiece. It can be easily shown that the increase of the angle between the workpiece and the tool leads to the resultant of the pressure shifts to the trailing edge.

Analytical solution of equation (4) is impossible even for a simple configuration between workpiece and tool. Therefore, it is appropriate to use numerical simulations.

Numerical simulation was performed in an Ansys Fluent environment. The entry conditions were chosen to match the experiment. The angle between the workpiece and the tool, which could not be measured during the experiments, was changed in four steps to describe the trend.

2. Experiment

2.1 Conditions

The whole experiment took place in a laboratory with a constant temperature of 24 °C. A 200 mm diameter tool with glued 0.58 g / cm^3 polyurethane was used on the NLP 400 HS-1. The density of the Auerpol PZ 110 polishing slurry used was 1.04 g/cm^3. To reduce the number of variables during polishing, the tool speed was set to a constant value of 50 rpm. Likewise, the rotation speed of the eccentric arm was set to a constant value of 5 rpm. The magnitude of the lens oscillation also remained unchanged throughout. The measurements were performed in eight positions of the tool relative to the workpiece $|r_a - R|$ = (-40; -30; -20; -10; 0; 10; 20; 30 mm). The positions are marked in Fig. 4.

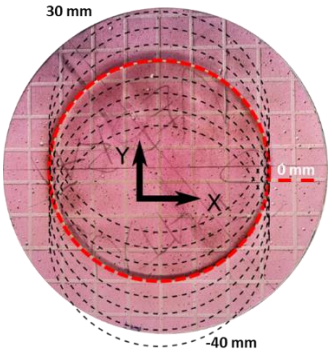

Fig. 4. Different Tool-Workpiece positions.

2.2 Preparation of the sample

The shape of the surfaces was polished based on previous experience with polishing to the best possible level in the preparatory phase of the experiment (Fig. 5. The surface form accuracy was checked with a Xonox VT 1200 PS Fizeau interferometer. The reference surface used was a Xonox PRO Line 4" transmission sphere with a focal length at infinity. The use of a 4 "sphere made it possible to evaluate the entire surface of the measured lens.

Subsequently, the lens was polished for 20 minutes in each position. After each measurement, the shape of the optical surface was measured, and the size of the removal was evaluated.

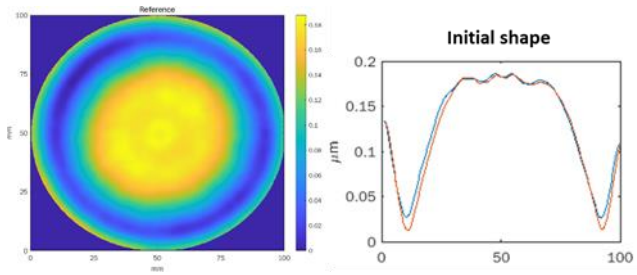

Fig. 5. Initial (before the experiment) shape of the surface.

3. Results

3.1. Experiment

Interferograms and profiles of the surface measured in perpendicular directions are presented at Fig. 6 and Fig. 7. All experiments were performed on the same surface. Change of the surface form after the polishing at specific position $(r_a - R)$are presented.

Results shows high removal rates at the edge of the surface for high values, positive or negative, of $(r_a - R)$. Position of $(r_a - R)$ close to 0 leads to increase of the removal rate at the centre of the workpiece.

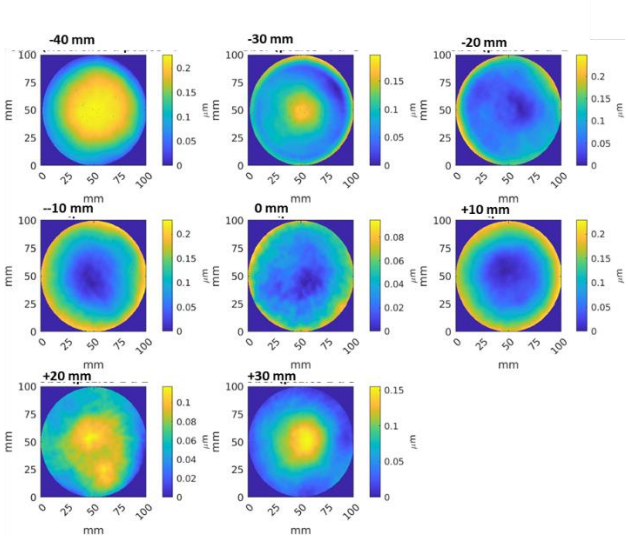

Fig. 6. Interferograms of the polished surface after individual steps. Removal after 20 minutes of polishing is presented for different values $(\boldsymbol{r_a - R})$.

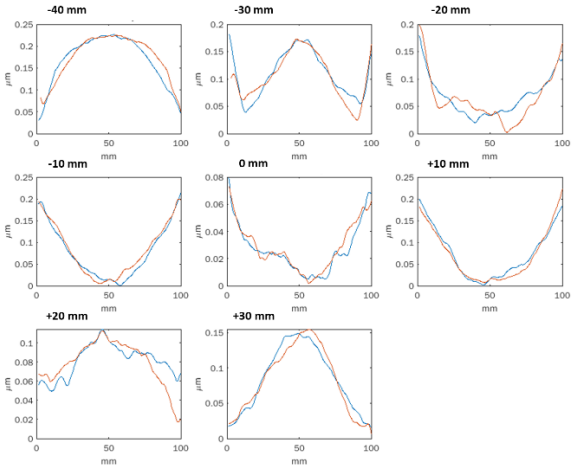

Fig. 7. Removal measured in perpendicular directions for different values of $(\boldsymbol{r_a - R})$.

3.2 Relative velocity

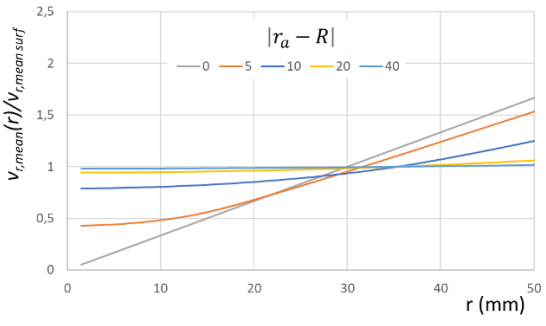

Fig. 8. Mean relative velocity during 50 cycles as a function of $|\mathbf{r_a - R}|$ and distance from the workpiece centre.

By analysing the equations (2), it was possible to evaluate the mean relative velocity at each workpiece point during a sufficiently long polishing time, which corresponds to 50 cycles of the overarm. The evaluation was performed

by numerical integration in the MATLAB environment. The results (Fig. 8) show that, except for states where $|r_a - R|$ is close to zero, the mean values of relative velocity are constant, independent on the position on the workpiece.
The unevenness increases whenω_w starts to me smaller than ω_t, which corresponds to the increasing friction in the ball joint.

3.3 Pressure distribution

The results of numerical simulations presented in Fig. 9 to Fig. 12 show the pressure distribution for different wedges and different values of $|r_a - R|$. The change in pressure as a function of angle is clear. The results also show a shift in the center of gravity of the pressure to the trailing edge with increasing angle.

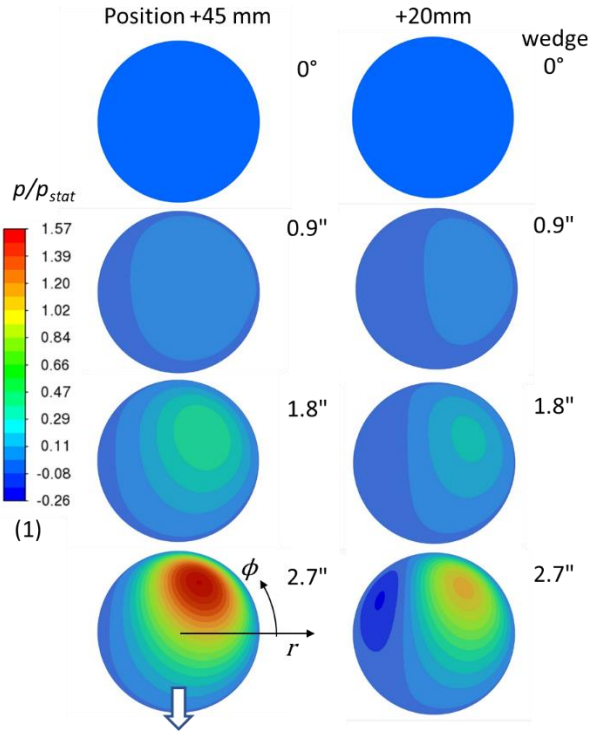

Fig. 9. Contour maps of the static pressure distribution on the workpiece. Position denotes $|\boldsymbol{r_a - R}|$.

4. Conclusion

The influence of the relative velocity and pressure distribution on the value of removal rate of material from the polished surface was analysed in the article. The analysis was compared with the experiment.

Based on the simple kinematics of the overarm mechanism it is possible to calculate the magnitude of the relative velocity and its mean value during the polishing process. It was shown that mean relative velocity increases significantly from the centre to the edge of the workpiece for small arm extension values. For higher values of $|r_a - R|$, the value of the mean relative velocity is independent of position and is almost uniform throughout the entire polished workpiece.

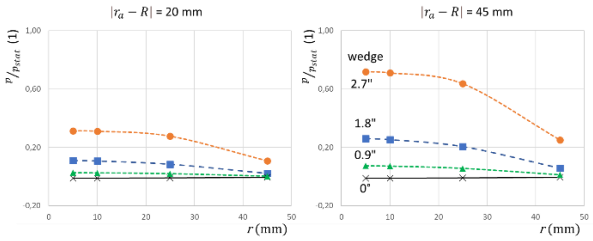

Fig. 10. Mean value of the static pressure as a function of the distance from the workpiece centre and the wedge.

A similar system can be used to analyse pressure. If there is no wedge between the workpiece and the tool, the static pressure on the workpiece surface will show only small differences. The pressure field can thus be considered homogeneous. However, the situation changes if the wedge starts to increase.

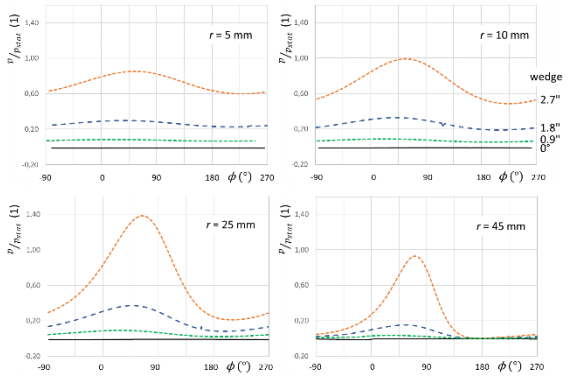

Fig. 11. Static pressure distribution at different positions on the workpiece for $|\boldsymbol{r_a - R}|$ = 45 mm.

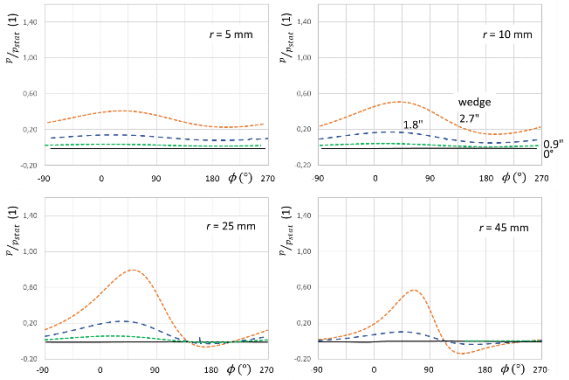

Fig. 12. Static pressure distribution at different positions on the workpiece for $|\boldsymbol{r_a - R}|$ = 20 mm.

Even a small value of the wedge leads to a significant change in the pressure distribution. As the wedge increases, the centre of the pressure shifts to the trailing edge. At the same time, the pressure increases.

The value of the wedge in the real process depends on the magnitude of the relative tool movement velocity, i.e., rotation speed of the tool and velocity of the overarm. So, it is possible to assume a higher value of dh when $|r_a - R|$ increases.

The results of the numerical simulations show a significant increase in pressure in the centre of the polished surface with increasing wedge (i.e., with

increasing $|r_a - R|$). If we consider both the effect of relative velocity and the effect of pressure, we conclude that it is possible to explain the results of the experiments as follows:

- At $|r_a - R|$ close to 0, an increase in the relative velocity from the center of the wafer is noticeable. On the contrary, there is no wedge between the workpiece and the tool, which leads to an even pressure distribution. Removal rate is therefore higher at the edge of the workpiece than at the centre (states -20; -10; 0; 10 at Fig. 7)

- At large $|r_a - R|$, the relative velocity is evenly distributed. On the contrary, the pressure shows a significant decrease from the centre to the edge. According to (), therefore, there is a significantly greater removal in the centre of the polished area (states -40; -30; +20; +30 at Fig. 7).

The presented results are only of a qualitative nature. In the next work, a detailed analysis will be performed using all the possibilities of CFD. At the same time, experiments will be performed in real processes with the most precisely defined conditions. From these first results, however, it is clear that CFD in combination with the experiment can provide a tangible explanation for such a complex phenomenon as polishing.

Acknowledgements

The research has been supported by the Ministry of Industry and Trade, project The Country for the Future, FX01030046.

References

1. N. Belkhir, D. Bouzid, V. Herold, Determination of the Friction Coefficient During Glass Polishing. Tribology Letters, 33, 55-61. (2008).
2. A. Kelm, R. Boerret, S. Sinzinger, Improving the polishing accuracy by determining the variance of the friction coefficient. Journal of The European Optical Society - Rapid Publications, 7. (2012)
3. F. W. Preston, The Theory and Design of Plate Glass Polishing Machines, J. Soc Glass Technology, Vol. 11, pp. 214-256. (1927)
4. C. J. Evans, E. Paul, D. Dornfeld, D. A. Lucca, G. Byrne, M. Tricard, F. Klocke, O. Dambon, B. A. Mullany, CIRP Annals, Volume 52, Issue 2 (2003)
5. N. Kyungyoon, L. Jiun-Yu, N. Saka, J.-H. Chun, Mechanics, Mechanisms and Modeling of the Chemical Mechanical Polishing Process. (2003).